THE JOURNAL OF COMPARATIVE NEUROLOGY 257:149-159 (1987)

Relationships Between Ganglion Cell Dendritic Structure and Retinal Topography in the Cat

J.D. SCHALL AND A.G. LEVENTHAL
Department of Anatomy, University of Utah School of Medicine, Salt Lake City, Utah 84132

ABSTRACT

The morphology of ganglion cell dendritic trees varies across the cat retina. Evidence is presented that the variation in two attributes of ganglion cell dendritic structure can be accounted for by specific aspects of the topography of the adult and developing retina.

The first attribute considered was the displacement of the center of the dendritic field from the cell body in the plane of the retina. The results of this study provide evidence that most ganglion cell dendritic fields are displaced away from neighboring cells, i.e., down the retinal ganglion cell density gradient. Because of the systematic dendritic displacement locally, the centers of the dendritic fields are arranged in a more precise mosaic than are their cell bodies.

The second attribute considered was the elongation and orientation of the dendritic fields. From approximately embryonic day 50 to postnatal day 10 the cat retina undergoes a process of maturation (reviewed by Rapaport and Stone: *Neuroscience 11*:289–301, '84) that begins at the area centralis and spreads over the retina in a horizontally elongated wave. We found that the elongation and orientation of retinal ganglion cell dendritic fields is significantly correlated with the shape of the wave of maturation. The orientation of a dendritic field is not predicted by the direction of its displacement nor is it directly related to the distribution of neighboring retinal ganglion cells.

These results indicate that the displacement of a ganglion cell's dendritic field from its cell body results from mechanisms different from those responsible for the orientation of the dendritic field. Factors that may be responsible for these two attributes of ganglion cell dendritic morphology are discussed.

Key words: retinal ganglion cell, dendritic morphology, dendritic development

The dendritic structure of ganglion cells varies over the cat retina. Certain aspects of this variation are related to the topography of the retina. For example, cell body and dendritic field size increases as ganglion cell density decreases (Boycott and Wässle, '74). The purpose of this paper is to demonstrate the relation between two specific attributes of ganglion cell dendritic tree structure and the topography of the adult and developing retina.

The first attribute considered is the lateral displacement of the center of the dendritic field from the center of the cell body. Experimental evidence has been provided for competition beween ganglion cell dendrites (Linden and Perry, '82; Perry and Linden, '82; Eysel et al., '85; Ault et al., '85; Leventhal et al., '87). If competitive dendritic interactions are involved in normal ganglion cell development, then the dendritic field of the most ganglion cells should tend to be displaced from its cell body in the direction of lowest density. It has been proposed that dendritic interactions are responsible for the nonrandom arrangement of ganglion cell bodies (Wässle and Riemann, '78). If so, then the mosaic formed by the centers of the dendritic fields

Accepted August 20, 1986.

J.D. Schall's current address is Department of Brain and Cognitive Sciences, E25-634, M.I.T., Cambridge, MA 02139.

should be more precise than the mosaic formed by their cell bodies. This study provides evidence to support these predictions.

The second attribute considered is the elongation and orientation of the ganglion cell dendritic fields. The dendritic fields of all types of ganglion cells in cat retina are elongated, and most are oriented approximately radially, i.e., like the spokes of a wheel with the area centralis at the hub (Leventhal and Schall, '83). While several hypotheses have been proposed (Levick and Thibos, '82; Thibos and Levick, '85; Eysel et al., '85), the process by which ganglion cell dendritic fields develop this characteristic elongation and radial orientation is not presently known. Evidence will be presented that the displacement of the dendritic fields down the density gradient does not account for their elongation and orientation. It will be demonstrated that the elongation and orientation of ganglion cell dendritic fields in the cat retina are correlated with the geometry of retinal maturation.

MATERIALS AND METHODS

Subjects

Alpha- and beta-type ganglion cells were sampled from the retinae of 12 adult cats; some of these animals provided data for an earlier study (Leventhal and Schall, '83).

Electrophoretic injection

Adult cats were prepared for electrophoretic injections as described previously (Leventhal and Schall, '83). Under Nembutal anesthesia the subject's head was positioned in a stereotaxic apparatus, and the scalp, bone, and dura mater were removed from the appropriate regions. The cortex was protected with a 4% solution of agar in saline. The body temperature was maintained at 38°C. Neosynephrine retracted the nictitating membranes, and atropine dilated the pupils. Zero-power contact lenses protected the corneas from desiccation. The optic disks and areae centralis were projected onto a tangent screen 114 cm from the subject's retina.

Prior to all horseradish peroxidase (HRP) injections, penetrations using low impedance (1–3 MΩ) microcapillary electrodes filled with 4 M NaCl were made into the dorsal lateral geniculate nucleus (LGNd) to locate specific representations of the visual field. The positions of the receptive fields of cells encountered in these penetrations directed the placement of the injections. Once a satisfactory site was located, the recording electrode was replaced with a microcapillary electrode filled with 10% HRP in Tris-HCl buffer (pH 8.6) containing 1% dimethyl sulfoxide (DMSO). Accurate positioning of this electrode was confirmed by recording prior to the injection. HRP was injected using currents of +3 μA (1.5 seconds on, 0.5 seconds off) for 2–3 hours. In some cats 3–5 HRP injections were made into the optic tract about 4 mm from the optic chiasm. The injections were spaced mediolaterally and extended from the ventral to the dorsal borders of the optic tract.

Histology and histochemistry

Subjects were maintained for 2 days following the HRP injections. Under deep anesthesia, each subject was perfused through the heart with 700 ml of lactated Ringer's solution containing 0.1% heparin, followed by 1,000 ml of 1% paraformaldehyde and 2.5% glutaraldehyde in 0.1 M phosphate buffer at pH 7.4, followed by 600 ml of lactated Ringer's solution containing 5% dextrose; all solutions were at 35°C. The brains were removed and the portions containing the injection sites were blocked and stored for 2–4 days in a 30% sucrose solution before frozen sectioning at 50 μm. The sections were collected in 0.1 M Tris-HCl buffer (pH 7.4), reacted for 20 minutes in 0.1 M Tris buffer containing 0.03% p-phenylenediamine dihydrochloride, 0.06% pyrocatechol, and 0.02% H_2O_2 (PPD-PC reagent) (Hanker et al., '77), and then transferred back into 0.1 M Tris-HCl buffer before mounting.

Whole retinae were removed and processed immediately after the perfusion. The retinae were rinsed in 0.1 M Tris buffer (pH 7.4) for 5 minutes, incubated in 1% cobalt chloride (Adams, '77) in Tris buffer containing 0.5% DMSO for 20 minutes, rinsed in Tris buffer for 5 minutes, rinsed in 0.1 M phosphate buffer (pH 7.4) for 5 minutes, prereacted in 0.1 M Tris buffer containing the PPD-PC reagent with 0.5% DMSO and no H_2O_2 for 15 minutes, reacted with fresh PPD-PC reagent containing 0.5% DMSO and H_2O_2 for 20 minutes and finally rinsed in phosphate buffer for 30 minutes; all reactions were carried out at 35°C. Photomicrographs of retinal ganglion cells illustrating the quality of the staining obtained using these procedures have been published (Leventhal, '82; Leventhal et al., '85).

Morphological analyses

Cells were drawn under the camera lucida using a final magnification of 225× or 562.5×. The drawing of each cell was traced onto a digitizing tablet interfaced to a PDP 11/23 computer. The high resolution of the digitizing tablet (0.1 mm, Houston Instruments) provided for a very accurate representation of the dendritic field. Each dendritic tree was represented by a series of coordinate points; thicker, proximal trunks were represented by more points than were thin, distal twigs. The center of both the cell body and dendritic tree were determined by calculating the mean values of the coordinates representing the respective parts of the ganglion cell. The distance separating the center of the dendritic field from the center of the cell body projected into the plane of the retina was measured. The direction of displacement of the center of the dendritic field from the center of the soma was measured relative to the vertical meridian, which was determined from the distribution of labeled ganglion cells resulting from HRP injections into the LGNd or optic tract.

Only that part of the dendritic field ramifying in its specific sublamina of the inner plexiform layer (IPL) was considered in the analysis of orientation. The cell body and proximal trunk dendrites were excluded since electron microscopic reconstructions indicate that these support virtually no synapses (Kolb, '79; Stevens et al., '80). Vectors were drawn from the center of the dendritic field to each point comprising the dendritic field. The angle of each vector was defined relative to the vertical meridian. Since orientation was being determined, angles across the circle, e.g., 10° and 190°, were equivalent. The vectors were summed; the angle of the resultant vector gave the orientation of the dendritic field. The length of the resultant vector, termed *orientation bias*, provided a measure of how elongated the dendritic field was. Orientation biases range from 0 to 1 with 0 indicating a circular dendritic field. Previous investigations (Levick and Thibos, '82; Leventhal and Schall, '83) have demonstrated that dendritic fields with an orientation bias of at least 0.1 may be considered significantly elongated. A demonstration of the morphological analyses of an alpha ganglion cell dendritic field is shown in Figure 1.

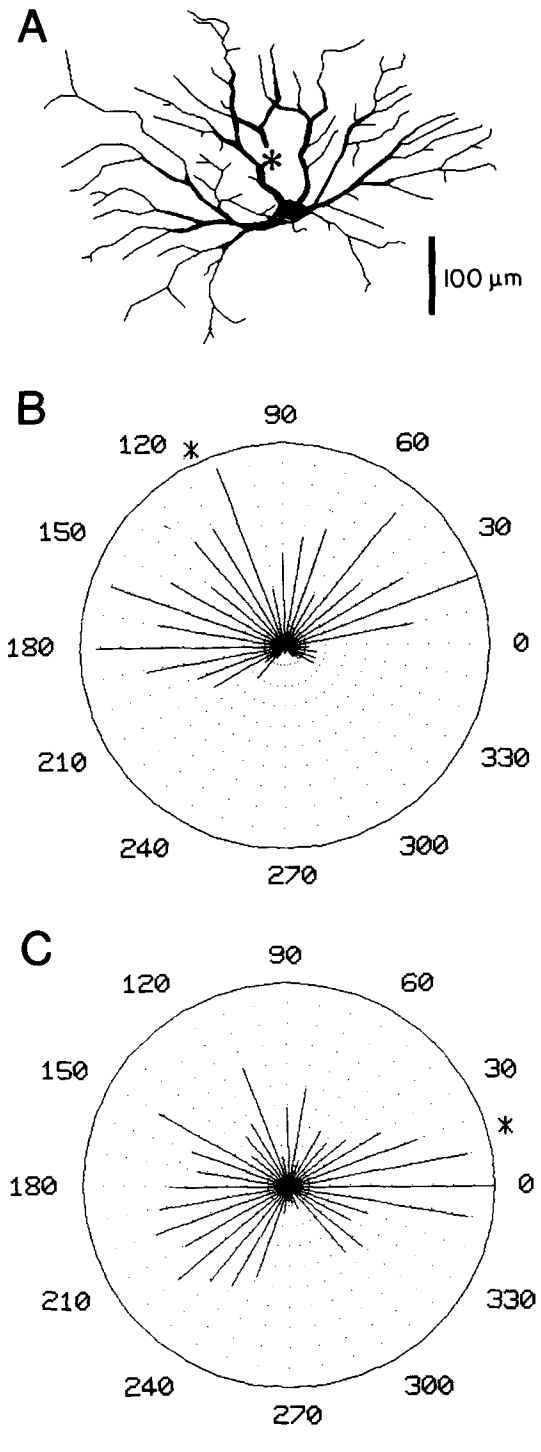

Fig. 1. A: Digitized representation of an alpha cell located superior to the horizontal meridian. The scale bar is aligned parallel to the vertical meridian of the retina. The asterisk is situated at the geometric center of the dendritic field. B: Circular histogram of the distribution of the dendritic field relative to the center of the cell body. Each line emanates from the coordinates of the center of the cell body; the length of each line is proportional to the amount of dendritic field in the given direction. The asterisk indicates the direction in which the center of the dendritic field is displaced from the center of the cell body. C: Circular histogram of the distribution of the dendritic field relative to the center of the dendritic field. The asterisk indicates the orientation of the dendritic field. Notice that the center of the dendritic field is displaced vertically from the cell body, but the dendritic field is oriented horizontally.

Patch analysis

The dendritic fields of all of the alpha cells in selected regions were drawn under camera lucida with a final magnification of 225×. Reducing the condenser setting on the microscope allows the outlines of cell bodies that are not filled with HRP to be seen (Leventhal, '82). Since alpha cell bodies are larger than any others in the ganglion cell layer, they can be identifed unambiguously. Only regions containing no unfilled alpha cells were chosen for this analysis. A computer replication of one of the patches has been published (Schall et al., '86b).

Ganglion cells whose dendritic fields ramify in the inner sublamina of the IPL, ON-center cells (Nelson et al., '78), appear to be distributed in a mosaic that is independent of the mosaic of ganglion cells whose dendrities ramify in the outer sublamina of the IPL, OFF-center cells (Wässle et al., '81a–c). In retinal wholemounts it is possible to distinguish between the depths of ramification of overlapping dendritic fields, so each dendritic field was assigned to either the ON or OFF sublamina.

A map of the ganglion cell bodies in each patch was drawn under camera lucida with a final magnification of 112.5×. The outline of each cell body in the map was traced onto the digitizing tablet; the Cartesian coordinates of the center of each cell body in a patch was stored. After determining the displacement of the center of the dendritic field from the center of its cell body, the dendritic field center could be placed in the map relative to the position of its cell body. By using the Cartesian coordinates representing the center of each cell body and dendritic field, the distance was measured from each cell body and dendritic field to the nearest cell body or dendritic field center, respectively.

Statistics

Specific statistical tests have been devised to analyze distributions of angles, and several such tests were utilized to analyze our data. A complete descrition of circular statistics can be found in Batschelet ('81). The *Rayleigh test* determines if a distribution of angles differs significantly from a random distribution, i.e., whether the angles cluster about some value in which case a high z value results. If a certain angle is expected, than the *V test* is a more powerful test of whether the distribution of angles is peaked about the expected value giving a high u value. To determine if the mean of a sample of angles was different from the expected angle, the confidence intervals given by Batschelet ('81) were used. *Watson's U^2 test* is a nonparametric comparison of two distributions to determine whether or not the two samples differ significantly; high U^2 values indicate a difference.

RESULTS

Magnitude of dendritic displacement

The distance in the plane of the retina between the geometric center of the dendritic field and the center of its cell body was measured for 573 alpha and beta ganglion cells across the cat retina. In Figure 2A the mean values of the dendritic displacement are shown as a function of eccentricity for alpha and beta cells; there was a significant tendency for the center of the dendritic field of ganglion cells to be displaced horizontally from the center of the cell body.

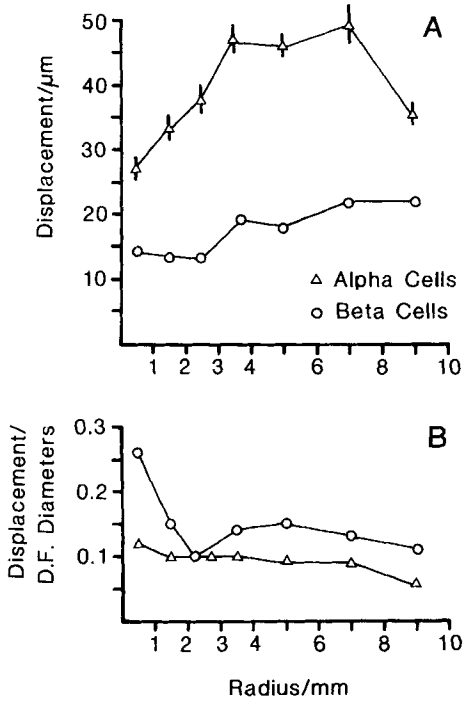

Fig. 2. A: Absolute dendritic displacement for alpha and beta cells as a function of eccentricity. The triangles represent the mean values of the displacement of the center of the dendritic field from the center of the cell body for alpha cells; the vertical bar represents the standard error. The circles represent the mean displacement of beta cell dendritic fields; the standard error at each eccentricity was smaller than the size of the symbol. Means were calculated for cells in 1-mm intervals within 4 mm of the area centralis and in 2-mm intervals therafter. Alpha cell dendritic fields are displaced from their cell bodies more than are beta cell dendritic fields, and the magnitude of displacement increases with eccentricity. B: Relative dendritic displacement for alpha and beta cells as a function of eccentricity. The distance in the horizontal plane of the retina betwen the center of the cell body and the center of the dendritic field was divided by the dendritic field diameter. The relative degree of displacement of alpha cell dendritic fields does not change with eccentricity. The relative dendritic displacement of peripheral beta cells is greater than that of alpha cells. Beta cell dendritic fields in the central 1 mm are displaced significantly more relative to their diameter than are their peripheral counterparts.

The magnitude of displacement tended to increase with eccentricity, more so for alpha than for beta cells. Since ganglion cell size increases with eccentricity, the increase in absolute dendritic displacement was not unexpected. Also, since alpha cells are larger than beta cells, it is not surprising that the displacement of the dendritic fields of alpha cells is greater than that of beta cells. It is of interest, therefore, to determine whether the degree of dendritic displacement relative to the size of the dendritic tree varies with eccentricity and across cell types. The magnitude of dendritic displacement was scaled to the size of the dendritic field by calculating the ratio of the magnitude of dendritic displacement divided by the diameter of the dendritic field. The mean values of this displacement ratio for alpha and beta cells are shown in Figure 2B. The relative dendritic displacement of alpha cells remained approximately constant with eccentricity. The relative dendritic displacement of beta cells more than 1 mm from the center of the area centralis also did not change appreciably with eccentricity and was significantly greater than the relative displacement of alpha cell dendritic fields. The relative dendritic displacement of beta cells in the area centralis, however, was significantly greater than that of their peripheral counterparts.

Direction of dendritic displacement

The angle difference was calculated between the direction of displacement of the center of a cell's dendritic field from its soma and the polar angle of the cell on the retina. A difference of 0° indicates displacement of the dendritic field from the soma toward the area centralis, and differences of ±180° indicate dendritic displacement toward the retinal margin, away from the area centralis. Outside the area centralis there appeared a systematic relationship between the direction of displacement of a ganglion cell's dendritic field from its cell body and its position on the retina. As shown in Figure 3, most dendritic fields more than 1 mm from the center of the area centralis were displaced from their cell bodies away from the area centralis, toward the retinal margin (mean angle = 172°, z = 34.9, $P < 0.001$).

Ganglion cell density varies over the cat retina. It is peaked at the area centralis and decreases toward the edge of the retina; along the horizontal meridian there is a ridge of elevated density which is the visual streak. The relationship between the direction of dendritic displacement of the alpha and beta cells and the direction of the ganglion cell density gradient at various locations on the retina is illustrated in Figure 4. The mean direction of dendritic displacement was calculated for the cells within 1 mm × 15° bins covering the retina and is represented by an appropriately inclined arrow. The direction in which the ganglion cell density slope was steepest was determined in each bin by measuring the angle of the line orthogonal to the ganglion cell isodensity contours in published ganglion cell density

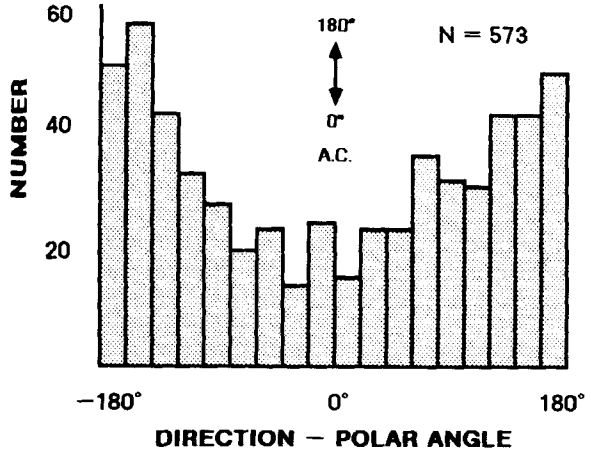

Fig. 3. Angle difference between the direction of displacement of the dendritic field from the cell body of alpha and beta ganglion cells more than 1 mm from the area centralis. Differences near 0° indicate that the dendritic field is displaced toward the area centralis, and differences near ±180° indicate that the dendritic field is displaced toward the retinal margin. Notice that the dendritic fields of most ganglion cells are displaced from their cell bodies away from the area centralis, toward the edge of the retina.

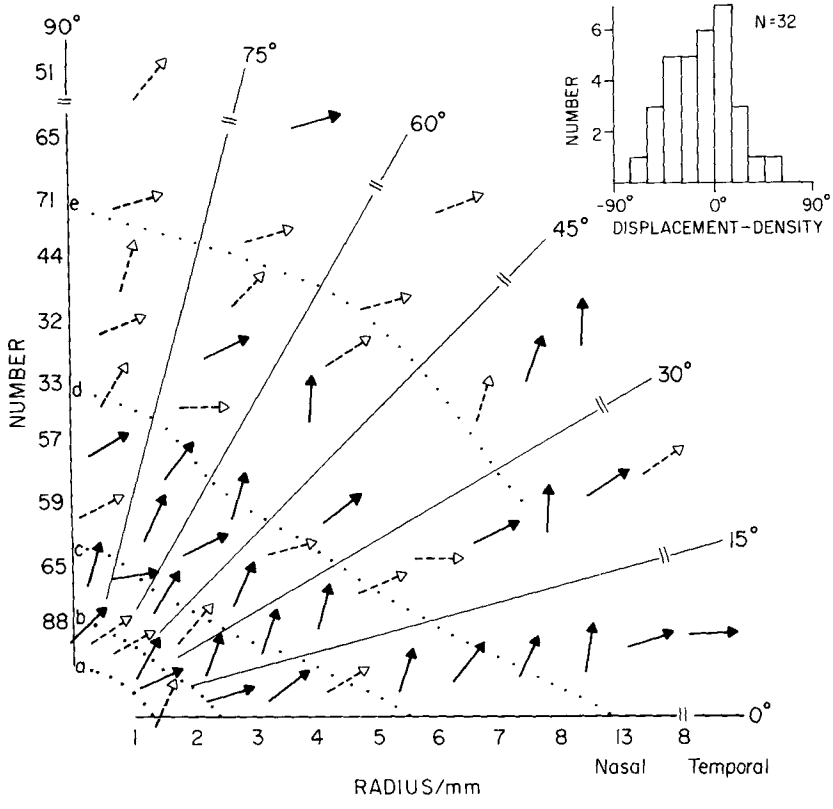

Fig. 4. Relationship between dendritic displacement and the ganglion cell density gradient. Each arrow represents the mean direction of displacement of the dendritic fields of the ganglion cells in 1 mm × 15° bins covering the retina; the mean directions of displacement of dendritic fields on the nasal and temporal edges are shown separately. Solid arrows signify that the distribution of displacement directions was significantly peaked (Rayleigh test with $P < 0.05$); dashed arrows were used otherwise; and no arrow was drawn in the bins containing fewer than three cells. The number of ganglion cells included at each radius is shown on the ordinate. Ganglion cell isodensity lines are superimposed on the figure; the values of density (cells/mm^2) represented by each line are as follows: a, 2,000; b, 1,000; c, 500; d, 250; and e, 125. The 125 cells/mm^2 isodensity line could not be completed owing to the change in scale on the abscissa representing the retinal margin. The differences between the mean direction of displacement and the direction of the steepest ganglion cell density gradient in each bin are shown in the histogram. Only those bins with significantly peaked distributions of displacement directions were included. Notice that most ganglion cell dendritic fields are displaced down the density gradient.

maps (Hughes, '75; Stone, '78).[1] It was evident that the dendritic fields of many ganglion cells were not displaced exactly away from the area centralis; for example, most dendritic fields in the visual streak were displaced away from the horizontal meridian. The angle difference between the direction of dendritic field displacement and the direction of the greatest ganglion cell density slope was calculated for each bin, and these values are shown in the histogram in Figure 4. The distribution is not flat (mean angle = −13°, u = 5.0, $P < 0.0005$), and the mean angle difference is not significantly different from 0° ($P < 0.05$). Thus, the direction of the ganglion cell density gradient predicts the mean direction of displacement of the ganglion cell dendritic fields from their cell body.

[1]The ganglion cell density maps published by Hughes ('75) and Stone ('78) differ somewhat with respect to the density in the visual streak. We analyzed our data using Hughes' and Stone's maps separately and found no significant differences. Consequently, the analyses presented used density values that were averaged from both maps.

Arrangement of dendritic field center

The spatial distribution of the cell bodies and dendritic field centers were analyzed in four groups of alpha cells. The first patch of cells extended 1 to 4 mm from the area centralis on the vertical meridian. The second patch covered from 2.5 to 4 mm from the area centralis on the vertical meridian. The third patch was 3 to 8 mm from the area centralis along the horizontal meridian. The fourth patch extended 8 to 11 mm from the area centralis on an oblique meridian. Figure 5 shows the disposition of some of the cells with dendritic fields ramifying in the OFF sublamina of one patch. The center of the dendritic field of most ganglion cells is displaced from the cell body toward the open area between other cells.

The mean and standard deviation of the separations of nearest neighbor cell bodies and cell dendritic field centers in each patch were calculated. The ratio of the mean to the standard deviation of the distribution of distances between nearest neighbors is a measure of the precision of spatial arrangement (Wässle and Riemann, '78). This ratio will be referred to as the *mosaic ratio*; the greater the *mosaic ratio*, the more precise the arrangement. In Table 1 these data are presented for the ON and OFF center ganglion cells in each patch. In the third column of the table are written the

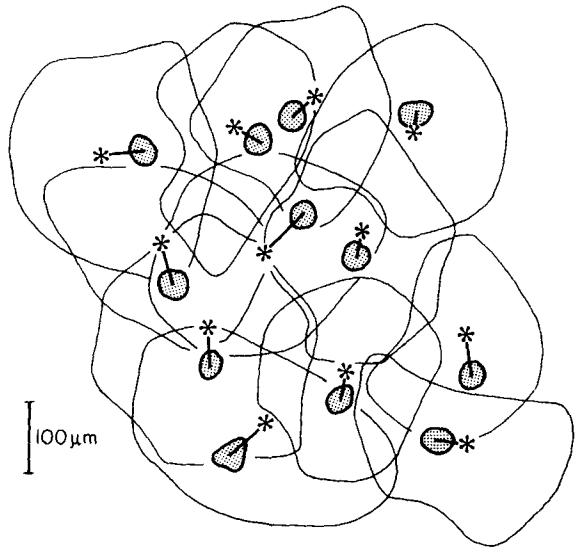

Fig. 5. Spatial arrangement of ganglion cell bodies and dendritic fields. This group of cells was included in patch number 1; the cells were approximately 3 mm from the area centralis on the vertical meridian. The dendritic fields of these cells ramified in the OFF sublamina of the inner plexiform layer. Notice that the dendritic field centers are displaced from their cell bodies into the open areas between other cell bodies; this results in the dendritic field center's being distributed in a more precise mosaic than are their cell bodies. In this small patch the *mosaic ratio* for the cell bodies was 3.90, and that for the dendritic field centers was 5.80.

differences between the *mosaic ratios* of the cell bodies and their dendritic field centers. In each case the *mosaic ratio* of the dendritic field centers is greater than that of the cell bodies.

Because the mosaic of ON and OFF center cells is more ordered than the mosaic of all the cells taken together, it has been suggested that the dendritic fields in the ON sublamina grow independently of those in the OFF sublamina (Wässle et al., '81a–c). If so, then the eight pairs of *mosaic ratios* (4 patches × 2 IPL levels) for the ON and OFF cell bodies and their dendritic field centers may be considered independent observations. With eight observations 2^8 or 256 outcomes are possible. The *mosaic ratio* for the dendritic field centers was greater than that of the cell bodies in each of the eight cases. The probability that this result occurred at random is 1 in 256 or 0.0039, which is unlikely.

TABLE 1. The Ratio of the Mean to the Standard Deviation of the Separations of the Nearest Neighbor Cell Bodies and Dendritic Field Centers in Each Patch[1]

	Cell bodies	Dendritic fields	Difference
Patch 1			
ON (n = 46)	3.62	4.83	+ 1.21
OFF (n = 55)	4.78	5.23	+ 0.45
Patch 2			
ON (n = 21)	3.03	3.18	+ 0.15
OFF (n = 26)	2.51	2.63	+ 0.12
Patch 3			
ON (n = 64)	3.59	3.83	+ 0.24
OFF (n = 71)	3.76	3.90	+ 0.14
Patch 4			
ON (n = 54)	3.61	4.27	+ 0.66
OFF (n = 62)	5.63	5.76	+ 0.13

[1]Cells ramifying in the ON and OFF sublaminae were considered separately and the number of cells is indicated. The differences between the values for the dendritic field centers and the cell bodies are written in the third column. Notice that in every case the mosaic ratio of the dendritic field centers is greater than that of the cell bodies.

Dendritic field orientation and the wave of maturation

From approximately embryonic day 50 (E50) to postnatal day 10 (P10) the cat retina undergoes a period of maturation (reviewed by Rapaport and Stone, '84). This maturation has been characterized by several separate features, including the appearance of the ganglion cell density gradient (Stone et al., '82), ganglion cell morphological differentiation (Rapaport and Stone, '83b), formation of the outer plexiform layer (OPL) (Rapaport and Stone, '82), and cessation of neurogensis (Rapaport and Stone, '83a). A similar phase of maturation has been observed in other species besides the cat, such as the rat (Webster and Rowe, '85), the rabbit (Stone et al., '85), and the human (Provis et al., '85). In the cat the process begins at the area centralis and expands over the retina in a horizontally elongated wave. As a first approximation the expanding region of maturity can be described as an ellipse. The expansion of such an ellipse at each point can be described by a vector whose angle and magnitude vary with polar angle as shown in Figure 6. This vector will be referred to as the *wave vector*. The wave vector is directed horizontally and is longest on the horizontal meridian and is vertical and shortest on the vertical meridian. Since the wave of maturation extends more horizontally than vertically, i.e., the horizontal component of the wave vector is greater than the vertical, the wave vector on the oblique meridians deviates from radial toward horizontal.

The relationship between the orientation of significantly elongated alpha and beta ganglion cell dendritic fields as defined previously (Leventhal and Schall, '83) and the angle of the wave vector is illustrated in Figure 7. The mean orientation of the ganglion cell dendritic fields within each 1 mm × 15° bin was calculated and is represented by a short, thick line. Rapaport and Stone ('82) illustrated the appearance of the OPL during retinal development; the average elongation of the mature region was 2.2. Using this value, the angle of the wave vector was calculated and was represented by a long, thin line. The angle difference was calculated between the mean orientation of the dendritic fields and the angle of the wave of maturation vector in each bin and these values are shown in the histogram in Figure 7. There was a significant correlation between the mean orientation of the dendritic fields in a spot of retina and the angle of the wave of maturation vector in that spot (mean difference = 0°, u = 8.09, $P < 0.0005$).

The angle difference was also measured between the mean orientation of the dendritic fields in each bin and the value of the polar angle of the bin. If the mean orientation was more horizontal than the polar angle, the angle difference was positive, and if the mean orientation was more vertical than the polar angle, the angle difference was negative. The mean angle difference between the mean orientations and the polar angles of each bin was +16°, which is significantly different from 0° ($P < 0.01$). Thus, polar angle did not predict dendritic field orientation as well as did the angle of the wave vector.

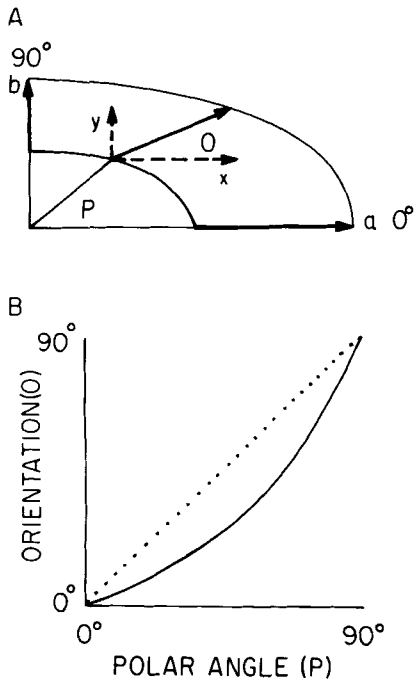

Fig. 6. **A:** An approximation of the geometry of the wave of maturation. The concentric ellipses in A represent the mature area at two times; the inner ellipse representing the earlier time. The expansion from the inner to the outer ellipse at any point can be described with a vector. The angle of the illustrated vector is given by $O = atan\ (y/x)$. The horizontal major axes of the ellipses extend a relative distance a, and the minor axes extend a distance b, so the elongation of the ellipse is given by $E = a/b$. For the illustrated ellipses $E = 2.2$, equal to the average elongation of the mature area illustrated in Figure 5 of Rapaport and Stone ('82). The horizontal component of the vector at a polar angle of P is given by $x = a \cdot cos(P)$, and the vertical component, by $y = b \cdot sin\ (P)$. Replace x and y such that $O = atan\ (b \cdot sin(P)/a \cdot cos(P))$. This expression can be simplified since $sin\ (P)/cos\ (P)$ equals $tan\ (P)$ and a/b equals E to give the equation that was used to estimate the angle through which the wave of maturation passes at a given polar angle, $O = atan\ (tan(P)/E)$. **B:** Vector orientation, O, plotted as a function of polar angle, P. If $E = 1$, then $O = P$ for all polar angles; this is shown by the dotted line. The wave of maturation, however, is horizontally elongated by a factor of 2.2. The orientation of the wave vector as a function of polar angle with $E = 2.2$ is shown by the solid line. In this case O is less than P except on the horizontal meridian ($P = 0°$) where $O = 0°$ and on the vertical meridian ($P = 90°$) where $O = 90°$.

Further evidence of the relationship between the ganglion cell dendritic orientation and the wave of maturation is obtained in comparing nasal and temporal retina. Since the wave of maturation is more elongated in nasal than in temporal retina (Rapaport and Stone, '82), the wave vector deviates horizontally more in nasal than in temporal retina. The horizontal deviation from radial of the dendritic field orientations is more pronounced in nasal than in temporal retina. The mean dendritic field orientation was not different from the angle of the wave vector in nasal (mean difference = 0°, u = 4.03, $P < 0.0005$) or temporal retina (mean difference = -5°, u = 4.05, $P < 0.0005$).

Dendritic field elongation and the wave of maturation

Some of the variation in ganglion cell dendritic tree elongation could be accounted for by changes with meridian. The mean orientation bias of dendritic fields sampled on the horizontal meridian was 0.27 (range 0.03 to 0.62 with a mode of 0.27); the average orientation bias of ganglion cells on the diagonal meridian was 0.22 (range 0.01 to 0.65 with a mode of 0.17); and that of cells on the vertical meridian was 0.20 (range 0.00 to 0.66 with a mode of 0.17). The distribution of orientation biases of dendritic fields on the horizontal meridian was significantly different from both the diagonal ($U^2 = 0.28$, $P < 0.001$) and vertical ($U^2 = 0.36$, $P < 0.002$) meridians. Thus, the dendritic fields in the visual streak are more elongated than the dendritic fields on the diagonal or vertical meridians. Since the mature region extends more along the horizontal meridian, less along the diagonal and least along the vertical meridian, the variation in ganglion cell dendritic elongation was qualitatively correlated with the variation of the relative magnitude of the wave of maturation.

Some of the variability in ganglion cell dendritic elongation could also be accounted for by the orientation of the dendritic field relative to the wave vector. The mean orientation bias for the dendritic fields oriented within 22.5° of the angle of the vector of wave of maturation was 0.25 (range 0.01 to 0.62; mode 0.27); the mean orientation bias for the dendritic fields oriented from 22.5° to 67.5° off of the angle of the wave vector was 0.20 (range 0.01 to 0.66; mode 0.17), and the mean orientation of the remaining ganglion cells was 0.18 (range 0.00 to 0.47; mode 0.17). The distribution of orientation biases for dendritic fields orientation within 22.5° of the angle of the wave vector is significantly different from the distribution of orientations biases for dendritic fields oriented more than 22.5° off of the angle of the wave vector ($U^2 = 0.59$, $P < 0.0001$). These differences were more pronounced in the visual streak and in nasal retina. Hence, throughout the retina dendritic fields that are oriented parallel to the angle of the vector of the wave of maturation were more elongated than dendritic fields oriented otherwise.

DISCUSSION

The major findings of this study are the following: 1) the center of the dendritic field of most alpha and beta ganglion cells is significantly displaced from the center of the cell body. The absolute magnitude of dendritic displacement increases with eccentricity and is greater for alpha than for beta cells. 2) The relative dendritic displacement of alpha and beta cells in peripheral retina is approximately constant and is greater for beta than for alpha cells; beta cell dendritic fields are displaced significantly more in the area centralis. 3) The dendritic fields of most ganglion cells in a spot of retina tend to be displaced down the slope of ganglion cell density in that spot of retina. 4) The centers of the dendritic fields are arranged in a more precise mosaic than are their cell bodies. 5) The mean orientation of the dendritic fields in a spot of retina can be predicted from the angle through which the wave of maturation passes in that spot of retina. 6) The elongation of the dendritic fields in a spot of retina is qualitatively related to the relative magnitude of the wave of maturation in that spot of retina.

Directed growth of dendritic fields

Previous investigators have noticed that the center of the dendritic field of many ganglion cells is normally displaced laterally from the center of the cell body (Leicester and Stone, '67; Honrubia and Elliott, '70; Boycott and Wässle, '74; Wässle et al., '81c). At least three events during retinal development might be responsible for the systematic dis-

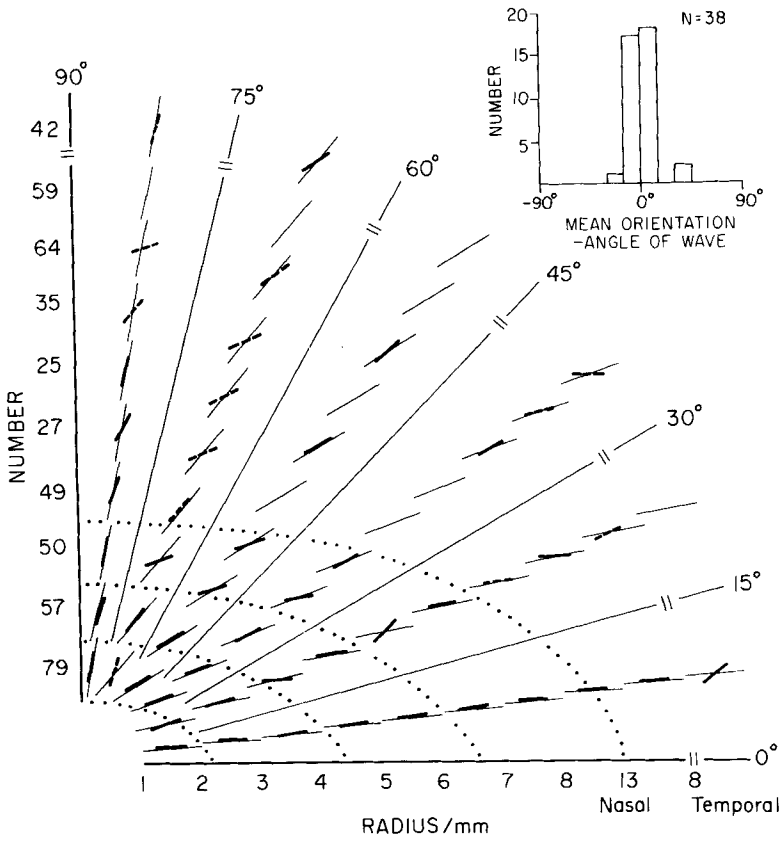

Fig. 7. Relationships between dendritic field orientation and the geometry of the wave of maturation. The thick lines represent the mean orientation of the significantly oriented alpha and beta cell dendritic fields in each 1 mm × 15° bin. Solid lines signify that the distribution of orientations was significantly peaked (Rayleigh test with $P < 0.05$); dashed lines were used otherwise, and no line was drawn in bins containing fewer than three cells. The number of dendritic fields included at each radius is shown on the ordinate; since only significantly elongated dendritic fields were included, the number of cells is less than that illustrated in Figure 4. The long, thin line in each bin represents the angle of the wave vector in each bin. The angles were calculated with the formula derived in Figure 4 using an elongation of 2.2; ellipses of this elongation are superimposed with dotted lines. The differences between the mean orientation of the dendritic fields in each bin and the angle through which the wave of maturation passes in that bin are shown in the histogram. The mean orientation of the dendritic fields in a region of retina is highly correlated with the angle through which the wave of maturation passes in that region.

placement of the ganglion cell dendritic fields from their somas down the ganglion cell density gradient: 1) transretinal migration of the cell bodies, 2) passive stretching of the retina, and 3) directed growth owing to dendritic competition.

Rowe and Dreher ('82) have reported that the dendritic fields of beta cells in the area centralis of the cat retina are displaced from their cell bodies toward the center of the area centralis. Although less prounced, such a pattern resembles the primate fovea, which appears to result through transretinal migration of the cell bodies away from the center of the fovea (Hendrickson and Kupfer, '76). As suggested by Rowe and Dreher, central cat beta ganglion cells may undergo a similar transretinal migration. Our finding that, relative to their dendritic field diameter, beta cell dendritic fields in the area centralis are displaced significantly more than their peripheral counterparts is consistent with this idea.

If transretinal migration can result in displaced dendritic fields in central retina, then it is possible that such is also the case in peripheral retina. The density gradient of ganglion cells may result from transretinal migration of initially uniformly distributed ganglion cell bodies toward the center of the retina and into the visual streak. Such migration would also result in the correlation we have observed between displacement and the density gradient if the dendritic fields do not move in the IPL. Recent evidence, however, indicates that the ganglion cell density gradient in cat retina is formed by mechanisms other than ganglion cell migration (Stone et al., '82). Hence, while transretinal migration of the ganglion cell bodies would not seem to be a plausible explanation of the observed dendritic displacement, it cannot be excluded at this time.

The displacement of dendritic fields from their cell bodies may be a consequence of passive stretching as the retina expands. Mastronarde et al. ('84) have shown that the ganglion cell layer expands nonuniformly. These authors report that there is relatively more radial expansion in central retina and more tangential expansion in peripheral retina. The degree of expansion of the IPL relative to the ganglion cell layer is not known. While passive stretching of a dendritic field could result in a degree of the displacement, the pattern of ganglion cell dendritic field displacement over the retina does not appear to correlate with the pattern of

retinal expansion. For example, within about 5 mm of the area centralis in the visual streak, Mastronarde et al. found that the retina expands radially, while the present results indicate that the dendritic fields are displaced more vertically, i.e., tangentially, from their cell bodies.

A variety of cells growing in vitro appear to explore their immediate environment through extended filopodia, and neurities extend where the filopodia attach (Letourneau, '75). Dendritic fields appear to grow according to a similar process of filopodial attachment (Skoff and Hamburger, '74; Vaughn et al., '74). The filopodia of cultured cells attach to other substrates better than to other cells; consequently, the initial lamellipodia outgrowth extends away from neighboring cells (Albrecht-Buehler, '76). Such a mechanism can explain the significant correlation between the direction of dendritic field displacement and the direction of the ganglion cell desnity gradient. During development the local ganglion cell density gradient may determine the direction in which the dendritic fields are ultimately displaced as the dendrites extend preferentially toward the least dense region.

Manipulating the density of ganglion cells in restricted areas of retina provides a test of this hypothesis. A small lesion near the optic disk in neonatal rat or kitten results in retrograde degeneration of the ganglion cells whose axons were transected; this results in a limited area of retina that is depleted of ganglion cells. The dendritic fields of ganglion cells on the border of such an evacuated region extend their dendrities into the area of reduced ganglion cell density (Perry and Linden, '82; Eysel et al., '85; Ault et al., '85; Leventhal et al., '87).

Wässle and Riemann ('78) suggested that dendritic interactions may be responsible for the development of the mosaic arrangement of ganglion cell bodies. Wässle et al. ('81b) showed that the dendritic trees of alpha cells cover the space between the cells very economically. The present finding that the dendritic field centers are distributed in a more precise mosaic than their cell bodies provides further evidence that dendritic interactions during development may be responsible for not only the complete but the uniform coverage of the retina with ganglion cell dendritic fields.

Oriented growth of dendritic fields

The dendritic fields of ganglion cells in the cat (Leventhal and Schall, '83), ferret (Vitek et al., '85), macaque (Schall et al., '86a), and human retina (Rodieck et al., '84) are elongated and approximately radially oriented relative to the area centralis or fovea. Since the elongation of ganglion cell dendritic fields in the cat retina corresponds to that of their receptive fields (Hammond, '74; Peichl and Wässle, '83), and most ganglion cells respond best to radially oriented stimuli (Levick and Thibos, '82), it seems likely that the structure of a ganglion cell's dendritic field confers upon the cell its physiological orientation sensitivity.

A sufficient explanation of ganglion cell dendritic field elongation and orientation must account for at least four observations. First, the dendritic fields are oriented with respect to the area centralis and not the optic disk or some other point. Second, most ganglion cell dendritic fields are not oriented exactly radially with respect to the area centralis, but are oriented more horizontally than their polar angle predicts. This horizontal deviation is more pronounced in nasal than in temporal retina. Third, the dendritic fields in the visual streak are more elongated than those outside of the streak. Fourth, dendritic fields that are oriented approximately radially (given the horizontal deviation) are more elongated than those oriented otherwise. At least four events of retinal development might account for the ganglion cell dendritic field elongation and orientation: 1) directed growth owing to competition, 2) formation of the mosaic, 3) passive stretching owing to retinal expansion, and 4) the wave of maturation which passes over the retina from E50 to P10.

Comparing Figures 4 and 7, it is evident that the direction of displacement does not correlate with the orientation of a dendritic field as exemplified by the cell in Figure 1. In the total sample of ganglion cells there is no correlation between the direction of dendritic displacement and the orientation of the dendritic field. These two features of ganglion cell dendritic morphology, therefore, probably develop independently. Thus, dendritic competition, which seems to be responsible for the systematic dendritic displacement, does not seem to account for dendritic field elongation and orientation.

As shown by Wässle et al. ('81b) and the present report, dendritic growth in the IPL results in the ganglion cell dendritic fields covering the retina completely and uniformly. It may be that the ganglion cell dendritic fields achieve their characteristic elongation and radial orientation as a consequence of forming the mosaic. If this were so, the elongation and orientation of a dendritic field ought to be predicted from its neighbrohood. Other than a mutual tendency to be oriented parallel to the angle of the wave vector, however, ganglion cell dendritic fields with similar orientations are not clustered in the retina (Schall et al., '86b). Furthermore, the precision of the mosaic decreases with eccentricity (Wässle and Riemann, '78), but the elongation and systematic orientation of ganglion cell dendritic fields do not change appreciably from 0.5 mm from the center of the area centralis to the retinal margin (Leventhal and Schall, '83). Hence, dendritic growth within the ganglion cell mosiac does not account for the elongation or systematic orientation of the dendritic trees.

Passive stretching of the dendritic fields postnatally because of expansion of the retina in cat also cannot be solely responsible for the elongation and approximately radial orientation of the dendritic fields (Mastronarde et al., '84). In the first place, the magnitude of expansion is insufficient to stretch the dendritic fields to the degree observed. In the second place, the pattern of expansion over the retina does not correspond to the observed pattern of orientations. For example, more than 5 mm from the area centralis the degree of tangential expansion exceed the degree of radial expansion, but dendritic fields from 0.5 mm from the area centralis to the retinal margin tend to be oriented radially. The expansion of the cat retina from E57 to maturity has been determined by Wong ('85); similar considerations indicate that passive stretching prenatally is also an insufficient explanation of the elongation and orientation of ganglion cell dendritic fields.

The retinogeniculate pathway in the cat undergoes a process of maturation beginning around E50. The number of axons in the optic nerve declines from the early elevated level (Ng and Stone, '82). During this period the afferents from each eye segregate in the LGNd (Shatz, '83) and superior colliculus (Williams and Chalupa, '82), and the ganglion cell terminal arbors elaborate in the LGNd (Sretavan and Shatz, '84). Also during this period a wave of maturation spreads over the retina (reviewed by Rapaport and

Stone, '84). This maturation has been characterized by the appearance of the ganglion cell density gradient (Stone et al., '82), ganglion cell morphological differentiation (Rapaport and Stone, '83b), development of the OPL (Rapaport and Stone, '82), and cessation of neurogenesis (Rapaport and Stone, '83a). This maturation appears in a centrifugal spatiotemporal gradient, which begins at the area centralis and expands in a horizontally elongated wave over the retina. A similar wave of maturation has been observed from P4 to P8 in the rat (Webster and Rowe, '85), from E28 to P5 in the rabbit (Stone et al., '85), and from E100 to E210 in the human (Provis et al., '85). It is also important to note that retinal ganglion cells in the cat do not achieve morphological maturity until at least 3 weeks postnatally (Rusoff and Dubin, '78).

Evidence has been provided in this study that the elongation and orientation of the ganglion cell dendritic fields in a spot of retina is highly correlated with the geometry of the wave of maturation in that spot of retina. Based on this evidence it may be hypothesized that the elongation and orientation of ganglion cell dendritic fields are related to the wave of maturation. This hypothesis has more explanatory power than the alternatives. Because the wave is initiated at the area centralis, the dendritic field orientation relative to the area centralis can be rationalized. The horizontal elongation of the wave in nasal and temporal retina also predicts quantitatively the horizontal deviation of the dendritic field orientations in both hemiretina. The greater relative magnitude of the wave along the horizontal meridian predicts the greater elongation and radial tendency of the dendritic fields in the visual streak. As the area of maturation nears the retinal margin, its shape becomes more variable. This appearance correlates with the slightly reduced radial tendency of ganglion cell dendritic fields observed near the edge of the retina (Leventhal and Schall, '83).

This hypothesis can be tested by analyzing the dendritic morphology of ganglion cells in the retinae of other species. A process of maturation similar to that observed in the cat occurs in the human retina (Provis et al., '85). The maturation is initiated at the macula and spreads in a horizontally elongated wave over the retina. The wave in the human retina, however, is not as elongated as that in the cat. The proposed hypothesis predicts that the dendritic fields of ganglion cells in the primate retina should be oriented more horizontally than radial, but the horizontal deviation should be less than that observed in the cat. This was not considered in an analysis of ganglion cell dendritic oriented in the human retina (Rodieck et al., '85). In the macaque retina, however, there is a significant tendency for the ganglion cell dendritic fields to be oriented more horizontally than their polar angle, and the deviation is less than that in the cat (Schall et al., '86a).

While there is a centrifugal gradient of development in the rat retina, the process of maturation is less defined spatially and occurs more rapidly than that in carnivore or primate retina (Webster and Rowe, '85; V.H. Perry, personal communication). In correspondence with the hypothesis, the dendritic fields of type I ganglion cells in the rat retina are not as elongated as those in cat or monkey, and there is no relation between dendritic field orientation and retinal position (Dreher et al., '85; Schall et al., '87).

The mechanism through which the elongation and orientation of retinal ganglion cell dendritic trees might be related to the wave of maturation is not presently clear. In vitro neurites extend preferentially parallel to an artificially oriented fibronectin substrate (Turner and Carbonetto, '84). It is possible that components of a substrate upon which ganglion cell dendrites grow are aligned parallel to the angle of the vector of the wave of maturation. Dendrites extending parallel to the orientation of the substrate may be facilitated, while dendrites growing otherwise may not extend as well. The interactions between dendrites presumably responsible for the displacement away from other dendritic fields may be superimposed on this elongated oriented growth.

CONCLUSIONS

The dendritic fields of most ganglion cells are displaced down the slope of the ganglion cell density gradient. The mosaic formed by the dendritic field centers is more precise than that of their cell bodies. Dendritic competition may be responsible for the observed displacement, but it does not account for the orientation and elongation of ganglion cell dendritic trees. Ganglion cell dendritic field elongation and orientation appears geometrically correlated with, and may, thererfore, depend on, the wave of maturation that passes over the retina from E50 to P10. The means by which dendritic tree growth is related to retinal maturation requires investigation.

ACKNOWLEDGMENTS

This work constitutes partial fulfillment of the requirements for the degree of Doctor of Philosophy for J.D.S. A preliminary report has been presented (Schall et al., '85). Support was provided by a Research Fellowship from the University of Utah Research committee to J.D.S. and by PHS grant EY04951 to A.G.L. We are grateful to V.H. Perry and J.M. Provis for their critical evaluation of the manuscript.

LITERATURE CITED

Adams, J.C. (1977) Technical considerations on the use of horseradish peroxidase as a neuronal marker. Neuroscience *2*:141.

Albrecht-Buehler, G. (1976) Filopodia of spreading 3T3: Do they have a substrate-exploring function? J. Cell Biol. *69*:275–286.

Ault, S.J., J.D. Schall, and A.G. Leventhal (1985) Experimental alteration of cat retinal ganglion cell dendritic field structure. Soc. Neurosci. Abstr. *11*:15.

Batschelet, E. (1981) Circular Statistics in Biology. New York: Academic Press.

Boycott, B.B., and H. Wässle (1974) The morphological types of ganglion cells of the domestic cat's retina. J. Physiol. (Lond.) *240*:397–419.

Dreher, B., A.J. Sefton, S.Y.K. Ni, and G. Nisbett (1985) The morphology, number, distribution and central projections of class I retinal ganglion cells in albino and hooded rats. Brain Behav. Evol. *26*:10–48.

Eysel, U.T., L. Peichl, and H. Wässle (1985) Dendritic plasticity in the early postnatal feline retina: Quantitative characteristics and sensitive period. J. Comp. Neurol. *242*:134–145.

Hammond, P. (1974) Cat retinal ganglion cells: Size and shape of receptive field centres. J. Physiol. (Lond.) *242*:99–118.

Hanker, J.S., P.E. Yates, C.B. Metz, and A. Rustioni (1977) A new specific, sensitive and non-carcinogenic reagent for the demonstration of horseradish peroxidase. J. Histochem. *9*:789–792.

Hendrickson, A., and C. Kupfer (1976) The histogenesis of the fovea in the macaque monkey. Invest. Ophthalmol. Vis. Sci. *15*:746–756.

Honrubia, F.M., and J.H. Elliott (1970) Dendritic fields of the retinal ganglion cells in the cat. Arch. Ophthalmol. *84*:221–226.

Hughes, A. (1975) A quantitative analysis of the cat retinal ganglion cell topography. J. Comp. Neurol. *163*:107–128.

Kolb, H. (1979) The inner plexiform layer in the retina of the cat: Electron microscopic observations. J. Neurocytol. *8*:295–329.

Leicester, J. and J. Stone (1967) Ganglion, amacrine and horizontal cells of the cat's retina. Vision Res. *7*:695–705.

Letourneau, P.C. (1975) Possible roles for cell-to-substratum adhesion in neuronal morphogenesis. Dev. Biol. *44*:77–91.

Leventhal, A.G. (1982) Morphology and distribution of retinal ganglion cells projecting to different layers of the dorsal lateral geniculate nucleus in normal and Siamese cats. J. Neurosci. *2*:1024–1042.

Leventhal, A.G., and J.D. Schall (1983) Structural basis of orientation sensitivity of cat retinal ganglion cells. J. Comp. Neurol. *220*:465–475.

Leventhal, A.G., J.D. Schall, and S.J. Ault (1987) Extrinsic factors determining retinal ganglion cell dendritic field structure in the cat. (in preparation).

Levick, W.R., and L.N. Thibos (1982) Analysis of orientation bias in cat retina. J. Physiol. (Lond.) *329*:243–261.

Linden, R., and V.H. Perry (1982) Ganglion cell death within the developing retina: A regulatory role for retinal dendrites? Neuroscience *7*:2813–2827.

Mastronarde, D.N., M.A. Thibeault, and M.A. Dublin (1984) Non-uniform postnatal growth of the cat retina. J. Comp. Neurol. *228*:598–608.

Nelson, R., E.V. Famiglietti, and H. Kolb (1978) Intracellular staining reveals different levels of stratification for on- and off-center ganglion cells in cat retina. J. Neurophysiol. *41*:472–483.

Ng, A.Y.K, and J. Stone (1982) The optic nerve of the cat: Appearance and loss of axons during normal development. Dev. Brain Res. *5*:263–271.

Peichl, L. and H. Wässle (1983) The structural correlate of the receptive field centre of alpha ganglion cells in the cat retina. J. Physiol. (Lond.) *341*:309–324.

Perry, V.H., and R. Linden (1982) Evidence for dendritic competition in the developing retina. Nature *297*:683–685.

Provis, J.M., D. Van Driel, F.A. Billson, and P. Russell (1985) Development of the human retina: Patterns of cell distribution and redistribution in the ganglion cell layer. J. Comp. Neurol. *233*:429–451.

Rapaport, D.H., and J. Stone (1982) The site of commencement of maturation in mammalian retina: Observations in the cat. Dev. Brain Res. *5*:273–279.

Rapaport, D.H., and J. Stone (1983a) The topography of cytogenesis in the developing retina of the cat. J. Neurosci. *3*:1824–1834.

Rapaport, D.H., and J. Stone (1983b) Time course of morphological differentiation of cat retinal ganglion cells: Influences on soma size. J. Comp. Neurol. *221*:42–52.

Rapaport, D.H., and J. Stone (1984) The area centralis of the retina in the cat and other mammals: Focal point for function and development of the visual system. Neuroscience *11*:289–301.

Rodieck, R.W., K.F. Binmoeller, and J. Dineen (1985) Parasol and midget ganglion cells of the human retina. J. Comp. Neurol. *233*:115–132.

Rowe, M.H., and B. Dreher (1982) Functional morphology of beta cells in the area centralis of the cat's retina: A model for the evolution of central retinal specializations. Brain Behav. Evol. *21*:1–23.

Rusoff, A.C., and M.W. Dubin (1978) Kitten ganglion cells: Dendritic field size at 3 weeks of age and correlation with receptive field size. Invest. Ophthalmol. Vis. Sci. *17*:819–821.

Schall, J.D., S.J. Ault, and A.G. Leventhal (1985) Relationships between ganglion cell dendritic field structure and retinal topography in the cat. Soc. Neurosci. Abstr. *11*:14.

Schall, J.D., V.H. Perry, and A.G. Leventhal (1987) Ganglion cell dendritic structure and retinal topography in the rat. J. Comp. Neurol. *257*:160–165.

Schall, J.D., V.H. Perry, and A.G. Leventhal (1986a) Retinal ganglion cell dendritic fields in old-world monkeys are oriented radially. Brain Res. *368*:18–23.

Schall. J.D., D.J. Vitek, and A.G. Leventhal (1986b) Retinal constraints on orientation specificity in cat visual cortex. J. Neurosci. *6*:823–836.

Shatz, C.J. (1983) The prenatal development of the cat's retinogeniculate pathway. J. Neurosci. *3*:482–499.

Skoff, R.P., and V. Hamburger (1974) Fine structure of dendritic and axonal growth cones in embryonic chick spinal cord. J. Comp. Neurol. *153*:107–148.

Sretavan, D., and C.J. Shatz (1984) Prenatal development of individual retinogeniculate axons during the period of segregation. Nature *308*:845–848.

Stevens, J.K., B.A. McGuire, and P. Sterling (1980) Toward a functional architecture of the retina: Serial reconstruction of adjacent ganglion cells. Science *207*:317–319.

Stone, J. (1978) The number and distribution of ganglion cells in the cat's retina. J. Comp. Neurol. *180*:753–772.

Stone, J., M. Egan, and D.H. Rapaport (1985) The site of commencement of retinal maturation in the rabbit. Vision Res. *25*:309–327.

Stone, J., D.H. Rapaport, R.W. Williams, and L. Chalupa (1982) Uniformity of cell distribution in the ganglion cell layer of prenatal cat retina: Implications for mechanisms of retinal development. Dev. Brain Res. *2*:231–242.

Thibos, L.N., and W.R. Levick (1985) Orientation bias of brisk-transient y-cells of the cat retina for drifting and alternating gratings. Exp. Brain Res. *58*:1–10.

Turner, D.C., and S.T. Carbonetto (1984) Model systems tor studying the functions of extracellular matrix molecules in muscle development. Expl. Biol. Med. *9*:72–79.

Vaughn, J.E., C.K. Henrikson, and J.A. Grieshaber (1974) A quantitative study of synapses on motor neuron dendritic growth cones in developing mouse spinal cord. J. Cell Biol. *60*:664–672.

Vitek, D.J., J.D. Schall, and A.G. Leventhal (1985) Morphology, central projections and dendritic field orientation of retinal ganglion cells in the ferret. J. Comp. Neurol. *241*:1–11.

Wässle, H., and H.J. Riemann (1978) The mosaic of nerve cells in the mammalian retina. Proc. R. Soc. Lond. [Biol.] *200*:441–461.

Wässle, H. B.B. Boycott, and R.-B. Illing (1981a) Morphology and mosaic of on- and off-beta cells in the cat retina and some functional considerations. Proc. R. Soc. Lond [Biol.] *212*:177–195.

Wässle, H., I. Peichl, and B.B. Boycott (1981b) Dendritic territories of cat retinal ganglion cells. Nature *292*:344–345.

Wässle, H., I. Peichl, and B.B. Boycott (1981c) Morphology and topography of on- and off-alpha cells in the cat retina. Proc. R. Soc. Lond. [Biol.] *212*:157–175.

Webster, M.J., and M.H. Rowe (1985) Development of retinal topography in albino and pigmented rat. Neurosci. Lett. *19*:S106.

Williams, R.W., and L.M. Chalupa (1982) Prenatal development of retinocollicular projections in the cat: An anterograde tracer transport study. J. Neurosci. *2*:604–622.

Wong, R.O.L. (1985) Ontogeny of the cat retinal ganglion cell layer. Doctoral Dissertation, Australian National University, Canberra.